ICIC Express Letters
Part B: Applications
Volume **7**, Number **3**, March **2016**

ICIC International ©2016 ISSN 2185-2766
pp. **679–686**

MULTI-OBJECTIVE OPTIMIZATION DESIGN OF VARIABLE-FREQUENCY INDUCTION MOTOR FOR CEILING FANS USING RESPONSE SURFACE METHODOLOGY

Sy-Ruen Huang[1] and Kuo-Hua Huang[2,3,*]

[1]Department of Electrical Engineering
[2]Ph.D. Program in Electrical and Communications Engineering
Feng Chia University
No. 100, Wenhua Road, Taichung 407, Taiwan
*Corresponding author: huangkh@mail.ncut.edu.tw

[3]Department of Electrical Engineering
National Chin-Yi University of Technology
No. 57, Sec. 2, Zhongshan Rd., Taichung 411, Taiwan

Received August 2015; accepted October 2015

Abstract. *This paper concerns a multi-objective optimization for an external rotor three-phase variable-frequency induction motor (VFIM), using response surface methodology (RSM) and finite element analysis (FEA). The quantities of interest, namely the efficiency, the starting torque and the peak torque, are maximized with respect to four design parameters in the stator and rotor mechanism of a VFIM. Subsequently, computer simulations are well validated by experimental means, and the presented ceiling fan motor is demonstrated as a superior candidate relative to a conventional split-phase induction motor in terms of efficiency.*
Keywords: Response surface methodology, Finite element analysis, Variable-frequency induction motor, Ceiling fans, Multi-objective optimal design

1. **Introduction.** Conventional ceiling fans using an external rotor split-phase induction motor are frequently seen indoors. In most cases, low cost and high slip motors are employed, accounting for the poor performance of ceiling fans [1]. In an attempt to reduce the electricity consumption, a brushless DC (BLDC) motor is a superior candidate for the operation of ceiling fans due to a high efficiency [2]. However, there remain a couple of problems in a BLDC motor, e.g., they are priced too high to be competitive, the inherent cogging torque problem and the demagnetization of the permanent magnet involved.

For energy efficiency purposes, the development and commercialization of high efficiency electric motors is required for applications to ceiling fans. An external rotor three-phase variable-frequency induction motor (VFIM) can take the place of split-phase induction and BLDC motors employed in ceiling fans, and gain a number of advantages, e.g., a best C/P ratio, a high efficiency, a lower pulsating torque and a low-level noise.

In literature, it is the first time that a ceiling fan motor is designed in such a way that the requirements of multi-objective optimization can be met using response surface methodology (RSM) [3-6] and finite element analysis (FEA). This paper is presented with a focus on the optimization of the efficiency, the starting torque and the peak torque with respect to the mechanisms of the stator and the rotor. Subsequently, the mathematic model is well validated by numerical and experimental means. As it turns out, the use of the presented ceiling fan motor does as expected save the energy consumption relative to a conventional split-phase induction motor.

2. Methodology.

2.1. Initial design of VFIM.

This paper concerns a three-phase external rotor variable-frequency induction motor with 12 poles and 36 slots. Figure 1 shows a cross-section view of a ceiling fan motor, and Table 1 gives the specifications of a typical VFIM. The goal of this work is to design an optimized motor configuration using a central composite design (CCD) in RSM. Four design parameters, each with five levels, are involved in the configuration optimization. As illustrated in Figure 2, parameter A refers to the width of stator teeth, parameter B refers to the width of rotor teeth, parameter C refers to the depth of the rotor end-ring, and parameter D refers to the skew angle of a rotor slot. Table 2 presents the parameter settings involved in RSM, where level 0 represents the initial design settings of a VFIM.

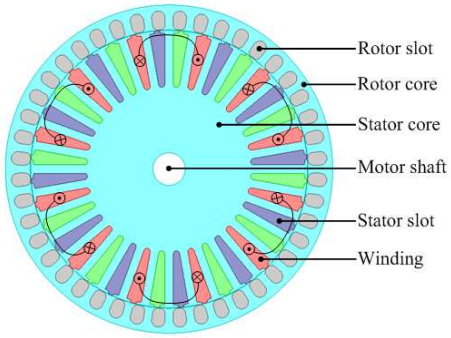

FIGURE 1. Cross section view of a typical VFIM

TABLE 1. Specifications of a typical VFIM

Items	Specification
Poles	12
Stator/Rotor slots	36/44
Rated speed (rpm)	190
Output power (W)	15
Operating frequency (Hz)	23
Winding layout	Concentrated winding
Rotor type	Squirrel cage
Stator diameter (mm)	171.7
Stator core length (mm)	20
Iron core material	H60
Wire diameter (mm)	0.45
Conductors per slot	180

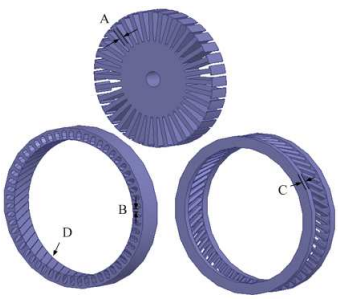

FIGURE 2. Design parameters A to D involved in a VFIM

Table 2. Parameter settings in RSM

Design Parameters	$-\alpha$	-1	0	1	$+\alpha$
A. Stator teeth width (mm)	3	3.5	4	4.5	5
B. Rotor teeth width (mm)	2.1	2.6	3.1	3.6	4.1
C. Rotor end-ring depth (mm)	5	6	7	8	9
D. Rotor slots skew angle (°M)	0	5	10	15	20

2.2. **Optimization method.** RSM is an optimization approach that combines a regression analysis, a statistical analysis and an experimental design. It is believed to be an optimization approach superior to a typical Taguchi method. Central composite design is the most common approach used in RSM [7], involving the following three types of experiments:

I. Factorial point experiment: since a second order model involves two interacting parameters, it is required to conduct 2^k factorial point experiments in a design optimization, where k represents number of parameters.

II. Axial point experiment: since a second order model takes into account a second order curvature, it is requested that two points be located at $\pm\alpha$ equidistant from the center point of an axis, that is, the end points of an axis. For multi-parameter optimization, let

$$\alpha = \sqrt[4]{G} \tag{1}$$

where G represents the number of the factorial point experiments.

III. Central point experiment: a central point experiment must be repeated for an acceptable variation in the values of predictive central points.

A regression analysis in RSM is given by Equations (2)-(4). The response parameters and the design parameters are related by

$$y = f(A, B, C, D : x_1, x_2, x_3, x_4) + error \tag{2}$$

where y denotes the output of the model, and x_1, x_2, x_3 and x_4 are the respective normalized design parameters of A, B, C and D. Then, for regression purposes, a second order polynomial approximation is given as

$$f(x_1, x_2, x_3, x_4) = \beta_0 + \sum_{i=1}^{k} \beta_i x_i + \sum_{i=1}^{k} \sum_{j=i+1}^{k} \beta_{ij} x_i x_j + \sum_{i=1}^{k} \beta_{ii} x_i^2 + \varepsilon \tag{3}$$

where β_0, β_i, β_{ij} and β_{ii} are estimated values, and ε is an estimated error. To determine the accuracy of a regression model, a coefficient of determination R^2, ranging between 0 and 1, is defined for significant certification. As R^2 approaches one, R^2 is given as

$$R^2 = \frac{SS_R}{S_{yy}} = 1 - \frac{SS_E}{S_{yy}} \tag{4}$$

where S_{yy}, the total variation of the response data with $n-1$ degrees of freedom, is computed as

$$S_{yy} = \sum_{i=1}^{n} (y_i - \bar{y})^2 \tag{5}$$

where y_i is an observed value, and $\overline{y}$ is the average of the observed values in the response, and the sum of the squared residuals, SS_E, is evaluated as

$$SS_E = \sum_{i=1}^{n} (y_i - \hat{y}_i)^2 \tag{6}$$

where $\hat{y}_i$ is a predicted value of the response. The sum of squares due to regression, SS_R, is evaluated as

$$SS_R = \sum_{i=1}^{n} (\hat{y}_i - \bar{y})^2 \tag{7}$$

The validity of a regression model is tested using an F test, defined as

$$F = \frac{SS_R/k}{SS_E(n-k-1)} \tag{8}$$

where k represents the number of the factors involved in the model, and n represents the total number of experiments.

3. **Design of Experiment.** Figure 3 shows a flowchart of a VFIM design. There are a total of 16 factorial point experiments involved in this paper, meaning that $\alpha = 2$ according to Equation (1). Table 3 presents the central composite design (CCD) of a VFIM, which covers 8 axial point experiments, 6 central point experiments in addition to the above-stated factorial point experiments, and gives FEM simulations on η, T_{st} and T_{peak} using Ansoft Maxwell 2D field simulator. Using Stat-Ease Design-Expert software, respective quadratic regression equations are given in Equations (9)-(11), and the corresponding coefficients of determination, R^2 can be found accordingly.

$$\begin{aligned}\eta = &+36.96 + 0.71 \cdot A - 0.055 \cdot B + 0.22 \cdot C - 1.96 \cdot D + 0.074 \cdot AB - 0.078 \cdot AC \\ &+ 0.27 \cdot AD + 0.026 \cdot BC - 0.14 \cdot BD + 0.24 \cdot CD - 0.13 \cdot A^2 \\ &- 0.026 \cdot B^2 - 0.053 \cdot C^2 - 0.91 \cdot D^2\end{aligned} \tag{9}$$

$$\begin{aligned}T_{st} = &+0.81 - 7.720E-003 \cdot A + 0.031 \cdot B - 0.051 \cdot C + 0.13 \cdot D + 4.573E \\ &-004 \cdot AB + 4.908E-004 \cdot AC - 4.225E-003 \cdot AD + 1.388E \\ &-003 \cdot BC + 8.560E-003 \cdot BD - 1.846E-003 \cdot CD + 1.621E \\ &-003 \cdot A^2 + 1.335E-003 \cdot B^2 + 7.582E-003 \cdot C^2 + 0.036 \cdot D^2\end{aligned} \tag{10}$$

$$\begin{aligned}T_{peak} = &+0.98 - 4.745E-003 \cdot A + 0.020 \cdot B - 0.033 \cdot C + 0.094 \cdot D + 9.431E \\ &-004 \cdot AB + 1.217E-004 \cdot AC - 2.927E-003 \cdot AD + 8.567E \\ &-004 \cdot BC + 6.896E-003 \cdot BD - 3.512E-003 \cdot CD + 1.314E \\ &-003 \cdot A^2 + 9.184E-004 \cdot B^2 + 5.720E-003 \cdot C^2 + 0.029 \cdot D^2\end{aligned} \tag{11}$$

TABLE 3. Output performances versus parameter settings in CCD for a VFIM

A	B	C	D	η (%)	T_{st} (N.m)	T_{peak} (N.m)	A	B	C	D	η (%)	T_{st} (N.m)	T_{peak} (N.m)
−1	−1	−1	−1	37.2246	0.7633	0.9459	1	1	1	1	35.3035	0.9668	1.0995
1	−1	−1	−1	38.0652	0.7567	0.9430	−2	−1	0	0	35.0094	0.8369	0.9986
−1	1	−1	−1	37.1279	0.8089	0.9732	2	1	0	0	37.7539	0.8102	0.9836
1	1	−1	−1	38.2755	0.8014	0.9704	0	−2	0	0	36.8409	0.7631	0.9519
−1	−1	1	−1	37.1643	0.6663	0.8881	0	2	0	0	36.7640	0.8817	1.0271
1	−1	1	−1	37.9370	0.6559	0.8797	0	0	−2	0	36.2706	0.9512	1.0762
−1	1	1	−1	37.3525	0.7141	0.9160	0	0	2	0	37.1155	0.7437	0.9412
1	1	1	−1	38.2039	0.7063	0.9117	0	0	0	−2	37.8753	0.6952	0.9022
−1	−1	−1	1	32.8396	1.0122	1.1301	0	0	0	2	28.6821	1.2254	1.3011
1	−1	−1	1	34.8221	0.9854	1.1117	0	0	0	0	36.9598	0.8147	0.9839
−1	1	−1	1	32.1839	1.0911	1.1844	0	0	0	0	36.9598	0.8147	0.9839
1	1	−1	1	34.5810	1.0620	1.1656	0	0	0	0	36.9598	0.8147	0.9839
−1	−1	1	1	33.9663	0.9038	1.0552	0	0	0	0	36.9598	0.8147	0.9839
1	−1	1	1	35.5257	0.8780	1.0356	0	0	0	0	36.9598	0.8147	0.9839
−1	1	1	1	33.3596	0.9849	1.1081	0	0	0	0	36.9598	0.8147	0.9839

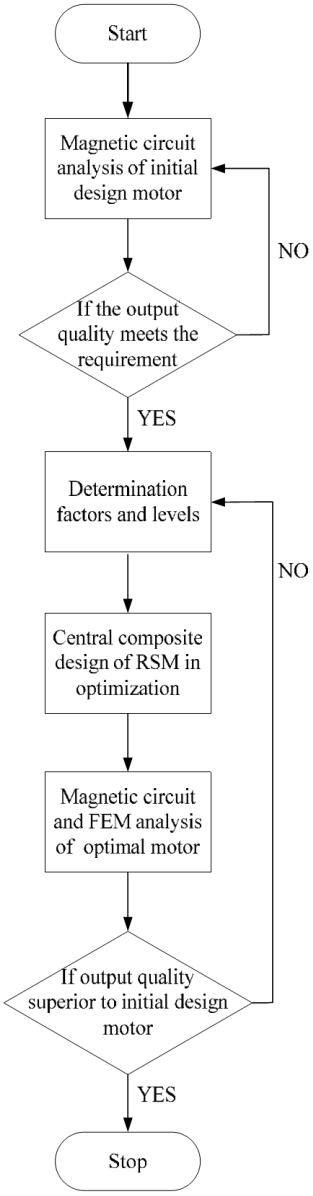

FIGURE 3. An optimized VFIM flow chart

TABLE 4. Parameter comparison between an initial and the optimized VFIM design

Parameter	***A* (mm)**	***B* (mm)**	***C* (mm)**	***D* (°M)**
Initial-VFIM	4	3.1	7	10
Optimal-VFIM	4.5	3.6	6	8.76

$R^2 = 0.9892$ ($F = 98.42$) indicates a 98.92% accuracy in the efficiency prediction by use of Equation (9), while $R^2 = 0.9992$ ($F = 1352.09$) and 0.9982 ($F = 593.23$) respectively indicate a 99.92% and 99.82% accuracy in the starting and the peak torque predictions by use of Equations (10) and (11). Table 4 gives a comparison between an initial and the optimized design parameters of a VFIM.

4. **Results and Discussion.** Using Maxwell 2D field simulator, simulated characteristic performances for an optimized VFIM are presented in Figures 4 to 6. Table 5 presents a simulated performance comparison between an initial and the optimized VFIM design. Figure 7 exhibits the respective photos of custom made stator and rotor for the optimal

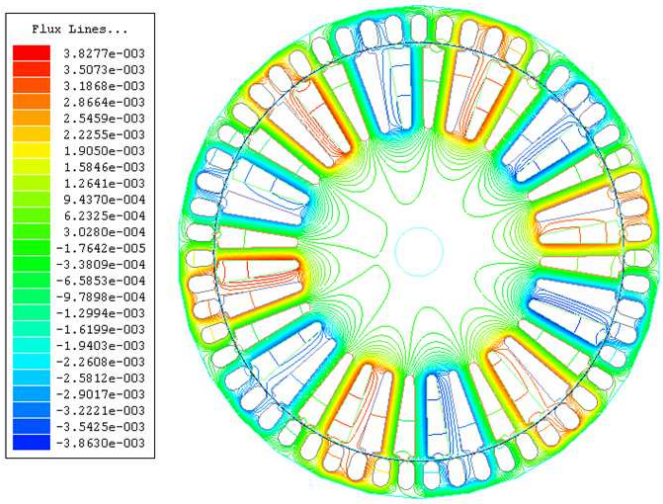

FIGURE 4. Flux line distribution inside a VFIM

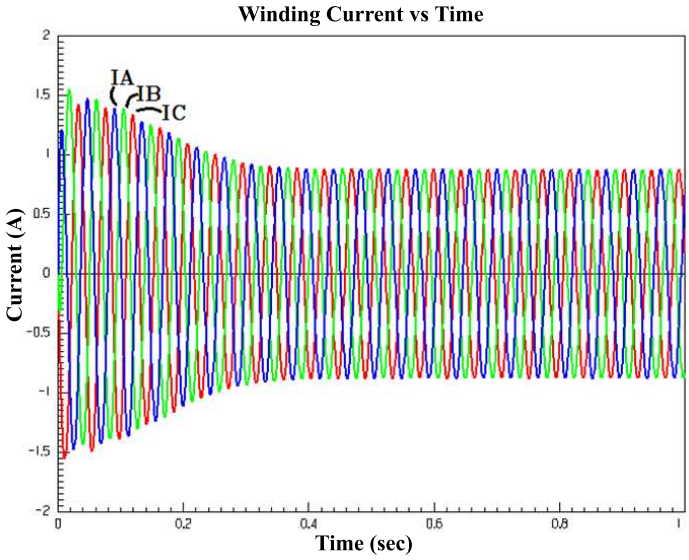

FIGURE 5. Simulated winding current waveform for a VFIM

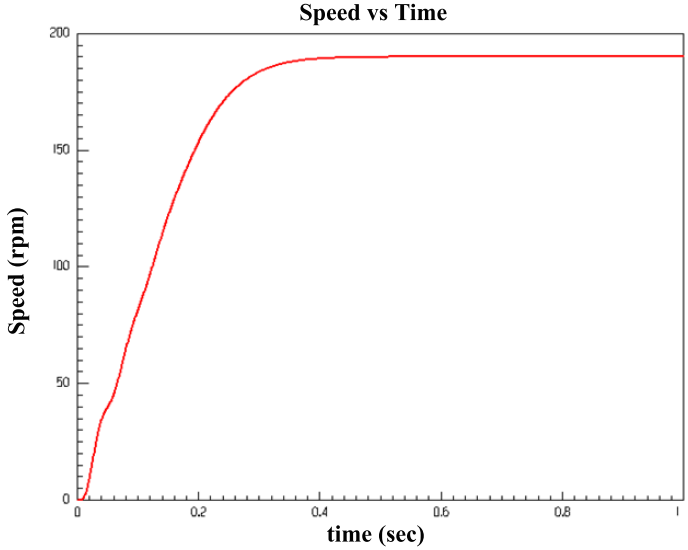

FIGURE 6. Simulated speed curve for a VFIM

TABLE 5. Simulated performance comparison between an initial and the optimized VFIM design

Motor type	η **(%)**	$\mathbf{T_{st}}$ **(N.m)**	$\mathbf{T_{peak}}$ **(N.m)**
Initial-VFIM	36.9598	0.8147	0.9839
Optimal-VFIM	37.5955	0.8713	1.0219

(a) (b)

FIGURE 7. Photos of (a) a custom made stator and winding, and (b) a rotor for an optimized VFIM

FIGURE 8. A test bed for a VFIM

TABLE 6. Test comparison between ceiling fans

Performance	**Split-Phase Induction motors**	**Optimal-VFIM**
T_{st} (N.m)	0.8	0.85
T_{peak} (N.m)	0.95	1
Consumption power (W)	63	47 (including a driver loss of 5W)

design, and Figure 8 demonstrates a photo of the built test bed for a VFIM. Table 6 presents a test comparison between ceiling fans, indicating that there is a 16 W reduction in the power consumption by the optimal design.

5. **Conclusions.** For energy efficiency purposes, the configuration of an external rotor three-phase variable-frequency induction motor is optimized for the use in ceiling fans. Multi-objective optimization, in terms of the efficiency, the starting torque and the peak torque, is done using RSM based on 2D FEM simulation, and the performance superiority is well validated by experimental means. It is found that a ceiling fan using an optimized VFIM consumes 25% less power than using a conventional split-phase induction motor. In the future, further research on replacing the aluminum rotor with the copper rotor to increase the performance of VFIM is suggested.

REFERENCES

[1] P. J. Holik, D. G. Dorrel and M. Popescu, Performance improvement of an external rotor split-phase induction motor for low-cost drive applications using external rotor can, *IEEE Trans. Magn.*, vol.43, pp.2549-2551, 2007.

[2] A. Saxena, Performance and cost comparison of PM BLDC motors for ceiling fan, *IEEE International Conference on Power Electronics, Drives and Energy Systems*, pp.1-5, 2014.

[3] B. H. Lee, K. S. Kim, J. P. Hong and J. H. Lee, Optimum shape design of single-sided linear induction motors using response surface methodology and finite-element method, *IEEE Trans. Magn.*, vol.47, pp.3657-3660, 2011.

[4] T. Ishikawa, M. Yamada and N. Kurita, Design of magnet arrangement in interior permanent magnet synchronous motor by response surface methodology, *IEEE Trans. Magn.*, vol.47, pp.1290-1293, 2011.

[5] B. H. Lee, J. P. Hong and J. H. Lee, Optimum design criteria for maximum torque and efficiency of a linear-start permanent magnet using response surface methodology and finite element method, *IEEE Trans. Magn.*, vol.48, pp.863-866, 2012.

[6] J. H. Lee, Optimum shape design solution of flux switching motor using response surface methodology and new type winding, *IEEE Trans. Magn.*, vol.48, pp.1637-1640, 2012.

[7] R. H. Myers and D. C. Montgomey, *Response Surface Methodology*, John Wiley and Sons, Inc., New York, 2002.